



Published in final edited form as:

Laryngoscope. 2014 March ; 124(3): 589–595. doi:10.1002/lary.24265.

Regional Peak Mucosal Cooling Predicts the Perception of Nasal Patency

Kai Zhao, Ph.D., Jianbo Jiang, Ph.D., Kara Blacker, Ph.D., Brian Lyman, Ph.D., Pamela Dalton, Ph.D., Beverly Cowart, Ph.D., and Edmund Pribitkin, M.D.

(KZ, JJ, KB, BL, PD, BC) Monell Chemical Senses Center, Philadelphia, USA and (KZ, BC, EP) Department of Otolaryngology, Thomas Jefferson University, Philadelphia, PA, USA

Abstract

Objective—Nasal obstruction is the principal symptom that drives patients with rhinosinus disease to seek medical treatment. However, patient perception of obstruction often bears little relationship to actual measured physical obstruction of airflow. This lack of an objective clinical tool hinders effective diagnosis and treatment. Previous work has suggested that the perception of nasal patency may involve nasal trigeminal activation by cool inspiratory airflow; we attempt to derive clinically relevant variables following this phenomenon.

Study design—Prospective healthy cohort.

Methods—Twenty-two healthy subjects rated unilateral nasal patency in controlled room air using a visual analog scale, followed by rhinomanometry, acoustic rhinometry and butanol lateralization thresholds (BLT). Each subject then immediately underwent a CT scan, enabling the construction of a “real-time” computational fluid dynamics (CFD) nasal airway model, which was used to simulate nasal mucosa heat loss during steady resting breathing.

Results—Among all measured and computed variables, only CFD-simulated peak heat loss posterior to the nasal vestibule significantly correlated with patency ratings ($r=-0.46$, $p<0.01$). Linear discriminant analysis predicted patency categories with 89% success rate, with BLT and rhinomanometric nasal resistance being two additional significant variables. As validation, CFD simulated nasal resistance significantly correlated with rhinomanometrically measured resistance ($r=0.41$, $p<0.01$).

Conclusion—These results reveal that our noses are sensing patency via a mechanism involving localized peak nasal mucosal cooling. The analysis provides a strong rationale for combining the individualized CFD with other objective and neurological measures to create a novel clinical tool to diagnose nasal obstruction and to predict and evaluate treatment outcomes.

Keywords

Nasal congestion; nasal obstruction; TRPM8; nasal cooling; cool perception; nasal trigeminal sensitivity

Introduction

Nasal sinus disease is one of the most common medical conditions in the US, accounting for 12.5 million physician office visits annually and an annual health expenditure of \$5.8 billion

Corresponding author: Kai Zhao, Monell Chemical Senses Center, Philadelphia, PA 19104, 267-519-4935 (phone and fax), kzhao@monell.org.

Conflicts of interest: “none.”

(National Health Interview Survey 2009, CDC). Among its major symptoms, nasal obstruction is the one that most often drives patients to seek medical treatment. However, since the early 19th century, doctors have been baffled by the inconsistent correlation between the nasal obstruction reported by patients and the observed physical obstruction to nasal airflow. Objective measurements, such as rhinomanometry, acoustic rhinometry, endoscopic examination, and CT staging scores often poorly or inconsistently correlate with patient perceptions^{1, 2}. Without validated objective clinical tools, the current diagnosis and treatment of nasal obstruction symptoms are based mostly on subjective opinion and patient feedback, which often results in inconsistent outcomes.

On the other hand, the perception of nasal patency clearly involves activation of nasal trigeminal cool afferents by inspiration of cool ambient air³. Pharmacologic modulation of trigeminal afferents has been shown to alter patency perception. For example, topical application of local anesthetics results in an artificial sensation of nasal obstruction, presumably due to blocking of the trigeminal afferents⁴, whereas topical application of menthol produces the illusion of decongestion and improved nasal airflow without actually altering nasal morphology⁵. Indeed, menthol had been widely used in common cold medications, nasal sprays, candy, chewing gum, and cigarettes long before its target receptor, the non-selective voltage-dependent cation channel TRPM8, was identified^{6, 7}. It is now known that when combined with cool air, menthol greatly enhances TRPM8 activation and perceived coolness⁸. Our previously published study⁹ experimentally isolated the various stimuli and physical determinants of the sensory percept of nasal patency and demonstrated that the perception of nasal patency in healthy individuals can be modulated, in part, by air temperature and humidity. The results further posited mucosal cooling as the underlying factor contributing to the sensation of nasal patency. Clinical evidence indirectly suggests that altered sensory input may play a role in the sensation of nasal obstruction; for example, patients with complete turbinectomies may still complain of nasal congestion despite exhibiting very little objective nasal resistance (“empty nose syndrome”, “atrophic rhinitis”)¹⁰. Despite these lines of evidence, no clinically applicable variables in this pathway have been identified.

The challenge lies in how to explain the differing perceptions of nasal patency among individuals, when, in most daily situations, we are exposed to common ambient air with similar temperature and humidity levels. The dynamic of cooling (heat loss) is not just a function of the static air temperature or humidity in the environment; it also depends on the interaction between an individual’s nasal airway structures and the inspired airflow. As a consequence, differences in individual nasal structure may result in different degrees of mucosal heat loss and thus lead to different experiences of nasal patency for different individuals.

Unfortunately, the nasal cavity is too small to allow detailed in vivo measurement of how various nasal anatomical changes and mucosal swelling may affect air/nasal mucosa interaction/cooling. However, studies evaluating mucosal detection sensitivity to air puffs^{11–13} and to chemical and electric stimulation^{14, 15} have revealed significant site differences, despite being based on observations made in limited numbers of spatial locations. These outcomes suggest that the degree of regional mucosal variability warrants a careful and detailed investigation. Recently, computational fluid dynamics (CFD) techniques have allowed us to develop a method to rapidly (within a few days) translate a CT scan into an individual, anatomically accurate, 3-D numerical nasal model that can be used to predict regional airflow and air/nasal wall cooling with high spatial resolution^{16–20}.

In this study, we attempted to quantify on an individual basis, through the CFD technique, how nasal mucosal cooling contributes to an individual’s perception of nasal patency. CFD

has the potential to further identify the mucosal site(s) having the greatest impact on obstructive symptoms and thereby guide the modification of the nasal architecture through surgery or implants. Ultimately, combined with measurement of trigeminally mediated coolness sensitivity, such an approach could offer great promise for developing clinical tools to objectively evaluate and effectively treat the symptom of nasal obstruction.

METHODS

Subjects

This study is an extension of a previously published study⁹. From the 44 healthy volunteers who were recruited from the local population for the previous study, a subset of 22 subjects were also invited to undergo CT scans for CFD modeling. The subgroup consisted of 10 males and 12 females; 20 were Caucasian, 1 African American and 1 Asian American. Their ages ranged from 21 to 39 years, with a mean of 25.6, median of 24.5, and standard deviation of 4.84 years. Both studies were approved by the University of Pennsylvania institutional review board. Written informed consent was obtained from all volunteers. All of the participants underwent medical history screening to exclude preexisting nasal sinus disease, and both acoustic rhinometry and rhinomanometry were performed on all subjects to objectively confirm the absence of severe nasal obstruction.

The procedures (as described in Zhao et al, 2011⁹) are outlined briefly below:

Exposure and nasal patency ratings

The test session was conducted in an air-conditioned, well-ventilated testing room at the Monell Chemical Senses Center (Philadelphia, PA). Subjects rated nasal patency unilaterally with a visual analogue scale while sampling air from three facial exposure boxes that were ventilated with untreated room air, cold air, and dry air, respectively at 10 L/min (see Figure 1); during sampling, in random order, a foam nose plug was used to occlude the untested nostril. The whole procedure was repeated twice, and the two ratings for each condition were averaged. Only the rating in the untreated room air condition was used in the current investigation, as we focused on the condition where individuals commonly experience obstructive symptoms. The effects of air humidity and temperature on nasal patency have been previously analyzed and published.

Rhinometry measurement

The unilaterally minimum (narrowest) cross-sectional area (MCA) in the anterior 5 cm of nasal airway was collected for each subject by acoustic rhinometry (SRE21000, RhinoMetrics A/S, Denmark). Nasal resistance²¹ during normal breathing was measured unilaterally by anterior rhinomanometry (SRE21000, RhinoMetrics A/S, Denmark) at a reference pressure drop of 75 pascals.

Nasal trigeminal lateralization thresholds

Unilateral lateralization detection thresholds for butanol were obtained by using an objective, two-alternative, forced-choice, modified staircase method²². Butanol was diluted in a series of 15 binary dilution steps: the first step contained 50% butanol dissolved in mineral oil; the next step, 25% butanol; the next step, 12.5%; and so on. . Butanol concentrations in the head space of each dilution bottle were measured and calibrated with gas chromatography. On each trial, the subject sniffed with both nostrils simultaneously from a pair of bottles: one contained a blank (10 ml of mineral oil), and one contained appropriately diluted butanol, and were then asked to identify which nostril received butanol. As previously described⁹, a scheme is applied to obtain unilateral thresholds based on the sequence of the subject's correct and incorrect responses.

CT scan, CFD model and Nasal heat loss simulation

After finishing the tests described above, participating subjects were immediately escorted by staff to Thomas Jefferson University Hospital (Philadelphia, PA), via a 10-minute subway ride, to undergo a spiral sinus CT. The CT enabled the construction of “real-time” CFD nasal airway models for each subject using methods described previously (Zhao *et al.* 2004). In brief, first the interface between the nasal mucosa and the air was delineated (using AMIRA®) on the scans (see Figure 2). Then, the nasal cavity air space was filled with tetrahedral elements (ICEMCFD®). A finer mesh (prism layer) was created near the mucosal surface to more accurately model the rapidly changing near-wall air velocity and odorant concentration.

Next, inspiratory and expiratory quasi-steady laminar (Keyhani *et al.*, 1995; Zhao *et al.*, 2004) nasal airflow were simulated (Fluent©, Fluent Inc, USA) by applying a physiologically realistic pressure drop between the nostrils and the nasal pharynx. Total airflow rates under various pressure drops through the left and right nasal cavities were calculated by a surface integration of air velocity at the nostril planes. This represents a simulated nasal resistance, which can be compared to rhinomanometrically measured ones.

Finally, nasal mucosal heat loss was simulated during steady resting breathing by assuming a constant breathing effort (15 Pascal) and nasal wall temperature (35 °C)^{23–27}. Spatial smoothing filters (2mm, 4mm radius moving average or median filter) were applied to the mucosal heat loss map to remove potential numerical artifacts, and also to take into account the likely spatial integration of the trigeminal system (see Figure 3). In order to account for different types of epithelium and the likely enhanced evaporative cooling posterior to the nasal vestibule, nasal heat loss was analyzed at locations both within and posterior to the nasal vestibule.

Data Analysis—The major candidate independent variables included nasal resistance, MCA, butanol lateralization thresholds, total nasal heat loss, and peak heat loss in regions after various smoothing filters. These independent variable were correlated to nasal patency ratings. A linear discriminant analysis (LDA) was performed in which the combination of the independent variables was used to predict subjects’ patency rating categories: excellent patency, normal patency and obstructed patency. As this is a healthy group with a mean patency score of 2.1 and a standard deviation of 1.8, we considered those subjects rated below the mean: excellent (n = 25 nostrils), those within +1 sd of the mean: normal (n=11) and those above 1 sd of the mean: moderately obstructed (n=6). LDA provides a weighting of the importance of each independent variables, as well as an index of how accurately the variables in combination predict group membership.

Missing data—Butanol lateralization thresholds were not collected for 7 subjects in the early stage of the study. Rhinomanometry measurement was not correctly performed on one subject due to staff error. Both variables, when included in the analysis, reduced the sample size.

Results

Results show that among all the independent variables, only the peak nasal mucosal heat loss posterior to the nasal vestibule (Figure. 4b) correlates significantly to the perceived patency under room air conditions (Pearson $r = -0.46$, $p < 0.01$). Considering the potential variability within the subjective patency ratings (test-retest reproducibility, $r = 0.81$, $p < 0.01$), this peak heat loss/patency association accounts for a substantial portion of the remaining variance. Furthermore, we also found that this peak regional heat loss did not correlate with total nasal heat loss, nasal resistance, or MCA (although the last two

correlated significantly with total nasal heat loss, see Table 1); and that it is possible to have substantial total heat loss but relatively small peak heat loss (see Fig. 4d and green circled data points in Fig. 4a,b), as well as relatively small total heat loss but substantial peak heat loss (Fig. 4c, red circled data points). These findings indicate that it is not that these other objective variables are inaccurate, but rather that it is regional heat loss that primarily underlies the perception of patency. It should be noted that we reported previously (Zhao *et al.*, 2011) that if all test box conditions (dry, cold and room air) are included, the correlation between total nasal heat loss and nasal patency becomes significant; this reflects a condition effect and does not contradict our findings based on individuals' patency ratings in untreated room air conditions only. As validation, CFD simulated nasal resistance significantly correlated with acoustically measured nasal resistance ($r = 0.41$, $p < 0.01$).

Peak nasal heat loss values reported above were obtained after application of a 2mm moving average filter; values obtained with no filter or after the application of other filters correlated more poorly with nasal patency ratings (e.g., for the 4mm median filter, $r = 0.22$, $p > 0.05$). Although there is very limited information regarding the spatial organization of the trigeminal system within the nasal cavity, the somatosensory system in skin has been well characterized and shows remarkable spatial integration capacity, from 2 to 14 cm² depending on skin location²⁸. In addition to removing potential numerical artifacts, the 2mm spatial filter may well reflect the integration zones of the nasal trigeminal system.

LDA was performed using the standard (Manova) approach and showed that all variables combined predicted the rated patency categories with 89.29% of success rate (Wilks' Lambda: .48753 approx. $F(8,72) = 3.8897$ $p < .0007$, see Table 2). Peak heat loss posterior to the nasal vestibule was the most significant variable, followed by rhinomanometrically measured nasal resistance and butanol lateralization thresholds. The remaining variables did not contribute significantly (see Table 3). Since the inclusion of butanol lateralization thresholds substantially decreased the sample size ($n = 42$ to 28), we also examined the effect of removing butanol lateralization thresholds from the candidate variables; the LDA success rate dropped to 78.57%, with heat flux posterior to the vestibule still the most significant variable. We further reran the LDA analysis based on the same sample ($n = 28$) with and without butanol lateralization thresholds; the results (with butanol 89.3% and without 82.1%) indicate that different sample sizes do have an effect on LDA outcome, and butanol thresholds do improve the LDA success rate. These different analyses are summarized below:

Effect of butanol lateralization threshold and missing data

N= 28, with Butanol, 89%

N= 28, without Butanol, 82%

N= 42, without Butanol, 78%

Discussion

It is important to investigate nasal patency as a sensory percept in order to identify and differentiate the physical and sensory factors contributing to the sensation of nasal patency, including air temperature, humidity, mucosal heat loss, nasal resistance, and nasal trigeminal sensitivity. Previous results show that perceived nasal patency in a healthy cohort can be modulated by air temperature and humidity, which would suggest that mucosal cooling is an underlying factor contributing to the sensation of nasal patency. However, dynamic cooling (heat loss) is not just a function of the static air temperature or humidity in the environment; it also depends on the interaction between an individual's nasal airway structures and the inspired airflow. By analyzing individual nasal heat loss patterns through CT scan-based

CFD models, we have confirmed that a regional peak mucosal heat loss significantly contributes to nasal patency perception under controlled ambient conditions. This information sheds new light on our understanding of nasal obstruction: a constricted airway with an insufficient airstream, as we often think about physical nasal obstruction, obviously produces little cooling; however, wide nasal passages with the bulk of the airstream having little contact with the mucosal wall may also produce a smaller peak in mucosal cooling and, thus, the sensation of congestion. This may in part explain the conundrum of empty nose syndrome.

Our CFD model simulation shows peak nasal heat loss to be concentrated anteriorly (Figure 4, c and d), coinciding with reported maps of mucosal detection sensitivity to air puffs, which also peak anteriorly¹¹⁻¹³. This may reflect adaptive optimization to co-localize high trigeminal cool sensitivity in areas of greater heat loss. However, it is unclear why only peak heat loss posterior to but not within the nasal vestibule correlates significantly with the patency rating. One explanation might be due to the different types of epithelium that comprise the nasal mucosa: the nasal vestibule is lined with a stratified squamous epithelium that is moderately keratinized and histologically resembles skin (Mygind et al, 1982), whereas the post vestibule nasal wall changes into the respiratory mucous membrane, with high vascularization and water permeability. Thus, heat loss posterior to the nasal vestibule may be enhanced through evaporation and better circulation. However, when we try to simulate evaporation through CFD models with the assumption of an infinite water source at the nasal mucosa according to²⁹, the resulted combined cooling (including evaporative cooling) does not correlate with patency ratings. A more realistic mucosal boundary condition might be necessary to account accurately for evaporative heat loss, and we are in the process of refining such a model with additional experiments.

Using butanol lateralization thresholds to assess the general nasal trigeminal sensitivity is common in chemosensory research. Although trigeminal sensitivity to butanol did not correlate independently with patency ratings, when combined with peak heat loss and measured nasal resistance, it improved the classification accuracy of the LDA. There are several reasons why this measure of trigeminal sensitivity alone might not affect patency. First, we tested a healthy, young cohort, all of whom would be expected to have normal trigeminal sensitivity. Second, while trigeminal activation of TRPM8 receptors is known to mediate innocuous cooling, less is known about the mechanisms and neuronal subpopulations underlying detection of other volatile irritants, such as butanol. Volatile alcohols and aldehydes activate some but not all cool-sensitive neurons³⁰, which suggests the likely co-existence within some neurons of mechanisms that respond to both cool and butanol stimulation. However, it is unlikely that the TRPM8 receptor mediates responses to butanol. Thus, sensitivity to butanol may only partially reflect trigeminal sensitivity to heat loss. Mapping of mucosal sensitivity to menthol (similar to^{31, 32}) or to well-controlled air puffs or temperature probes might yield more robust correlations with patency.

The literature also supports the notion that the nasal trigeminal senses may undergo adaptive processes during acute or prolonged disease processes. Chronic occupational exposure to irritants such as acetic acid or acetone specifically decreases trigeminal sensitivity to those chemicals^{33, 34}, whereas conditions such as allergic rhinitis are associated with greater sensitivity to nociceptive stimuli such as carbon dioxide and acetic acid^{35, 36}. Benoliel et al³⁷ have shown that warm and electrical current perception thresholds were hypersensitized during the acute phase of rhinosinusitis but hyposensitized during chronic (>3 months) rhinosinusitis. Limited studies in an animal model show that several inflammatory mediators cause decreased nerve responses to cooling³⁸. However, there has been no direct documentation of the impact of nasal sinus disease and/or inflammation on trigeminal cool afferent pathways in humans. This question may have significant clinical relevance in light

of the findings in this study and in the literature: a patient with ongoing nasal inflammation may have an altered baseline nasal trigeminal sensitivity that could exacerbate their obstructive symptoms. Similarly, we should not completely dismiss the contribution of nasal resistance, which did not correlate independently with patency ratings but, when combined with other variables, did improve the classification accuracy.

Conclusion

Currently, clinicians are unable to validate clinical outcomes of patient perception of nasal obstruction through objective measures. **In this pilot clinical study, we demonstrate that computational fluid dynamic modeling of peak heat loss just posterior to the nasal vestibule correlates significantly with the subjective perception of nasal patency in normal healthy subjects.** Further larger clinical studies with stratified patient populations should lead to more significant advances in our ability to identify the mechanisms associated with the perception of nasal obstruction. We believe that it is likely in the future to be able to combine several objective variables, including nasal heat loss, nasal trigeminal sensitivity, and nasal resistance, to create a new paradigm to objectively diagnose nasal obstruction in clinical populations and predict and evaluate treatment outcomes.

Acknowledgments

We thank Mr. Yuehao Luo (Monell), Miss Jenifer Shusterman (summer intern) and Mr. Chris Klock (Monell) for assistance in data collection, and Drs. Bruce Bryant and Paul Wise (Monell) for scientific discussions. Funding support: NIH 5R03DC008187, NIH P50 DC00006760

Reference List

1. Lam, dj; James, KT.; Weaver, EM. Comparison of anatomic, physiological, and subjective measures of the nasal airway. *Am J Rhinol.* 2006; 20(5):463–470. [PubMed: 17063739]
2. Andre RF, Vuyk HD, Ahmed A, Graamans K, Nolst Trenite GJ. Correlation between subjective and objective evaluation of the nasal airway. A systematic review of the highest level of evidence. *Clin Otolaryngol.* 2009; 34:518–525. [PubMed: 20070760]
3. Eccles R. Nasal airflow in health and disease. *Acta Otolaryngol.* 2000 Aug; 120(5):580–595. [PubMed: 11039867]
4. Jones AS, Crocher R, Wight RG, Lancer JM, Beckingham E. The effect of local anaesthesia of the nasal vestibule on nasal sensation of airflow and nasal resistance. *Clin Otolaryngol.* 1987; 12:461–464. [PubMed: 3442947]
5. Eccles R, Jones AS. The effect of menthol on nasal resistance to air flow. *J Laryngol Otol.* 1983; 97(8):705–709. [PubMed: 6886530]
6. McKemy DD, Neuhauser WM, Julius D. Identification of a cold receptor reveals general role for TRP channels in thermosensation. *Nature.* 2002; 416:52–58. [PubMed: 11882888]
7. Peier AM, Moqrich A, Hergarden AC, et al. A TRP channel that senses cold stimuli and menthol. *Cell.* 2002; 108:705–715. [PubMed: 11893340]
8. Voets T, Owsianik G, Nilius B. TRPM8. *HEP.* 2007; 179:329–344.
9. zhao, k; blacker, k; luo, y; bryant, b; Jiang, J. Perceiving nasal patency through mucosal cooling rather than air temperature or nasal resistance. *Plos One.* 2011; 6(10):e24618. [PubMed: 22022361]
10. Moore GF, Freeman TJ, Ogren FP, Yonkers AJ. Extended follow-up of total inferior turbinate resection for relief of chronic nasal obstruction. *Laryngoscope.* 1985 Sep; 95(9 Pt 1):1095–1099. [PubMed: 4033334]
11. Clarke RW, Jones AS. the relative importance of temperature and tactile stimulation. *Clin Otolaryngol.* 1992; 17:388–392. [PubMed: 1458619]
12. Clarke RW, Jones AS. the distribution of nasal airflow sensitivity in normal subjects. *J of Laryngology and otology.* 1994; 108:1045–1047.

13. Wrobel BB, Bien AG, Holbrook EH, et al. Decreased nasal mucosal sensitivity in older subjects. *Am J Rhinol.* 2006; 20:364–368. [PubMed: 16871945]
14. Meusel T, Negoias S, Scheibe M, Hummel T. Topographical differences in distribution and responsiveness of trigeminal sensitivity within the human nasal mucosa. *Pain.* 2010 Nov; 151(2): 516–521. [PubMed: 20817356]
15. Scheibe M, Zahnert T, Hummel T. Topographical differences in the trigeminal sensitivity of the human nasal mucosa. *Neuroreport.* 2006 Sep 18; 17(13):1417–1420. [PubMed: 16932150]
16. Zhao K, Scherer PW, Hajiloo SA, Dalton P. Effect of anatomy on human nasal air flow and odorant transport patterns: implications for olfaction. *Chem Senses.* 2004 Jun; 29(5):365–379. [PubMed: 15201204]
17. Zhao K, Dalton P. The way the wind blows: implications of modeling nasal airflow. *Curr Allergy Asthma Rep.* 2007 May; 7(2):117–125. [PubMed: 17437682]
18. Naftali S, Rosenfeld M, Wolf M, Elad D. The air-conditioning capacity of the human nose. *Ann Biomed Eng.* 2005 Apr; 33(4):545–553. [PubMed: 15909660]
19. Wolf M, Naftali S, Schroter RC, Elad D. Air-conditioning characteristics of the human nose. *J Laryngol Otol.* 2004 Feb; 118(2):87–92. [PubMed: 14979942]
20. Lindemann J, Keck T, Wiesmiller K, et al. A numerical simulation of intranasal air temperature during inspiration. *Laryngoscope.* 2004 Jun; 114(6):1037–1041. [PubMed: 15179209]
21. Clement PA. Committee report on standardization of rhinomanometry. *Rhinology.* 1984 Sep; 22(3):151–155. [PubMed: 6505516]
22. Wysocki CJ, Cowart BJ, Radil T. Nasal trigeminal chemosensitivity across the adult life span. *Percept Psychophys.* 2003; 65(1):115–122. [PubMed: 12699314]
23. Zhao K, Scherer PW, Hajiloo SA, Dalton P. Effect of anatomy on human nasal air flow and odorant transport patterns: implications for olfaction. *Chem Senses.* 2004 Jun; 29(5):365–379. [PubMed: 15201204]
24. Zhao K, Dalton P. The way the wind blows: implications of modeling nasal airflow. *Curr Allergy Asthma Rep.* 2007 May; 7(2):117–125. [PubMed: 17437682]
25. Naftali S, Rosenfeld M, Wolf M, Elad D. The air-conditioning capacity of the human nose. *Ann Biomed Eng.* 2005 Apr; 33(4):545–553. [PubMed: 15909660]
26. Wolf M, Naftali S, Schroter RC, Elad D. Air-conditioning characteristics of the human nose. *J Laryngol Otol.* 2004 Feb; 118(2):87–92. [PubMed: 14979942]
27. Lindemann J, Keck T, Wiesmiller K, et al. A numerical simulation of intranasal air temperature during inspiration. *Laryngoscope.* 2004 Jun; 114(6):1037–1041. [PubMed: 15179209]
28. Darian-smith, I. Thermal Sensibility. In: Bethesda, B., editor. *Handbook of physiology. Section 1: The nervous system, vol II.* USA: Oxford University Press; 1981.
29. Naftali S, Rosenfeld M, Wolf M, Elad D. The air-conditioning capacity of the human nose. *Ann Biomed Eng.* 2005 Apr; 33(4):545–553. [PubMed: 15909660]
30. Inoue T, Bryant BP. Multiple types of sensory neurons respond to irritating volatile organic compounds (VOCs) ?calcium fluorimetry of trigeminal ganglion neurons. *Pain.* 2005; 117:193–203. [PubMed: 16043294]
31. Meusel T, Negoias S, Scheibe M, Hummel T. Topographical differences in distribution and responsiveness of trigeminal sensitivity within the human nasal mucosa. *Pain.* 2010 Nov; 151(2): 516–521. [PubMed: 20817356]
32. Scheibe M, Zahnert T, Hummel T. Topographical differences in the trigeminal sensitivity of the human nasal mucosa. *Neuroreport.* 2006 Sep 18; 17(13):1417–1420. [PubMed: 16932150]
33. Wysocki CJ, Dalton P, Brody MJ, Lawley HJ. Acetone odor and irritation thresholds obtained from acetone-exposed factory workers and from control (occupationally non-exposed) subjects. *Am Ind Hyg Assoc J.* 1997; 58:704–712. [PubMed: 9342830]
34. Dalton P, Dilks D, Hummel T. Effects of long-term exposure to volatile irritants on sensory thresholds, negative mucosal potentials, and event-related potentials. *Behav Neurosci.* 2006 Feb; 120(1):180–187. [PubMed: 16492128]

35. Shusterman D, Murphy MA, Balmes J. Differences in nasal irritant sensitivity by age, gender, and allergic rhinitis status. *Int Arch Occup Environ Health*. 2003 Oct; 76(8):577–583. [PubMed: 12920525]
36. Shusterman D, Murphy MA. Nasal hyperreactivity in allergic and non-allergic rhinitis: a potential risk factor for non-specific building-related illness. *Indoor Air*. 2007 Aug; 17(4):328–333. [PubMed: 17661929]
37. Benoliel R, Biron A, Quek SY, Nahlieli O, Eliav E. Trigeminal neurosensory changes following acute and chronic paranasal sinusitis. *Quintessence Int*. 2006 Jun; 37(6):437–443. [PubMed: 16752699]
38. Linte RM, Ciobanu C, Reid G, Babes A. Desensitization of cold- and menthol-sensitive rat dorsal root ganglion neurones by inflammatory mediators. *Exp Brain Res*. 2007 Mar; 178(1):89–98. [PubMed: 17006682]



Please rate the degree of nasal congestion you are currently experiencing when breathing in the face-box by placing a mark on the scale below:



Figure 1.
Air exposure boxes and the visual analog scale used in the study.

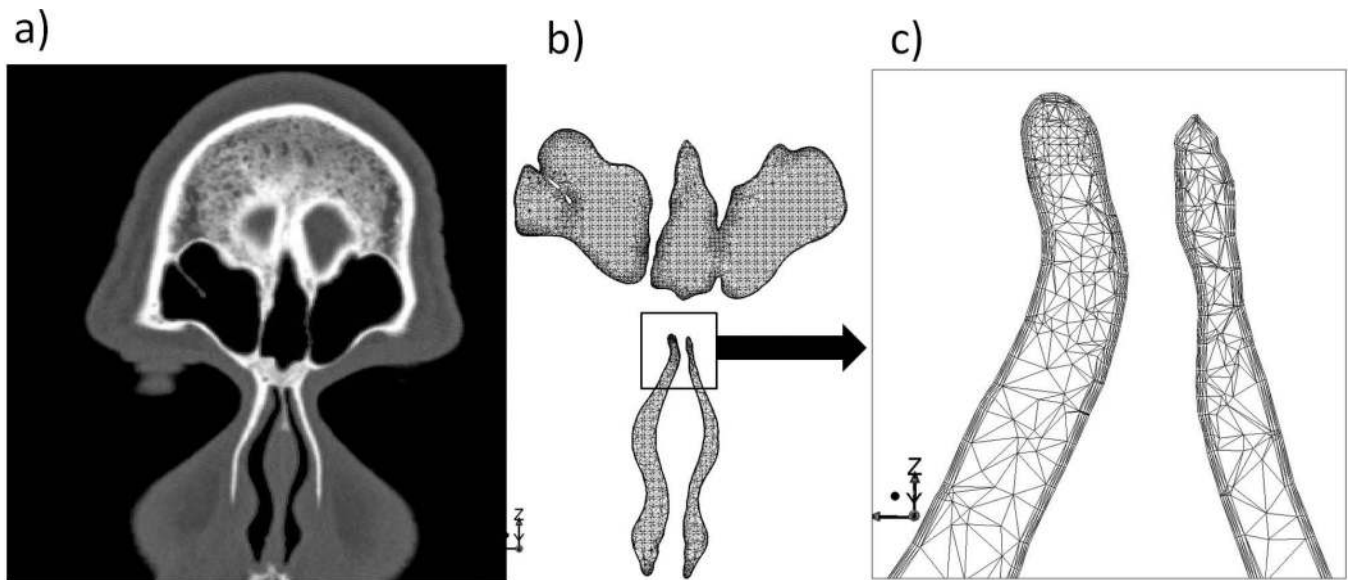


Figure 2. Coronal section of nasal CFD model for one subject (b) and the corresponding CT image (a). The whole nasal model consists of 3 million tetrahedral elements, with layers of small and fine elements along the wall (c, zoom in view), capturing accurately the rapid near-wall changes of air velocity, temperature and heat transfer profile.

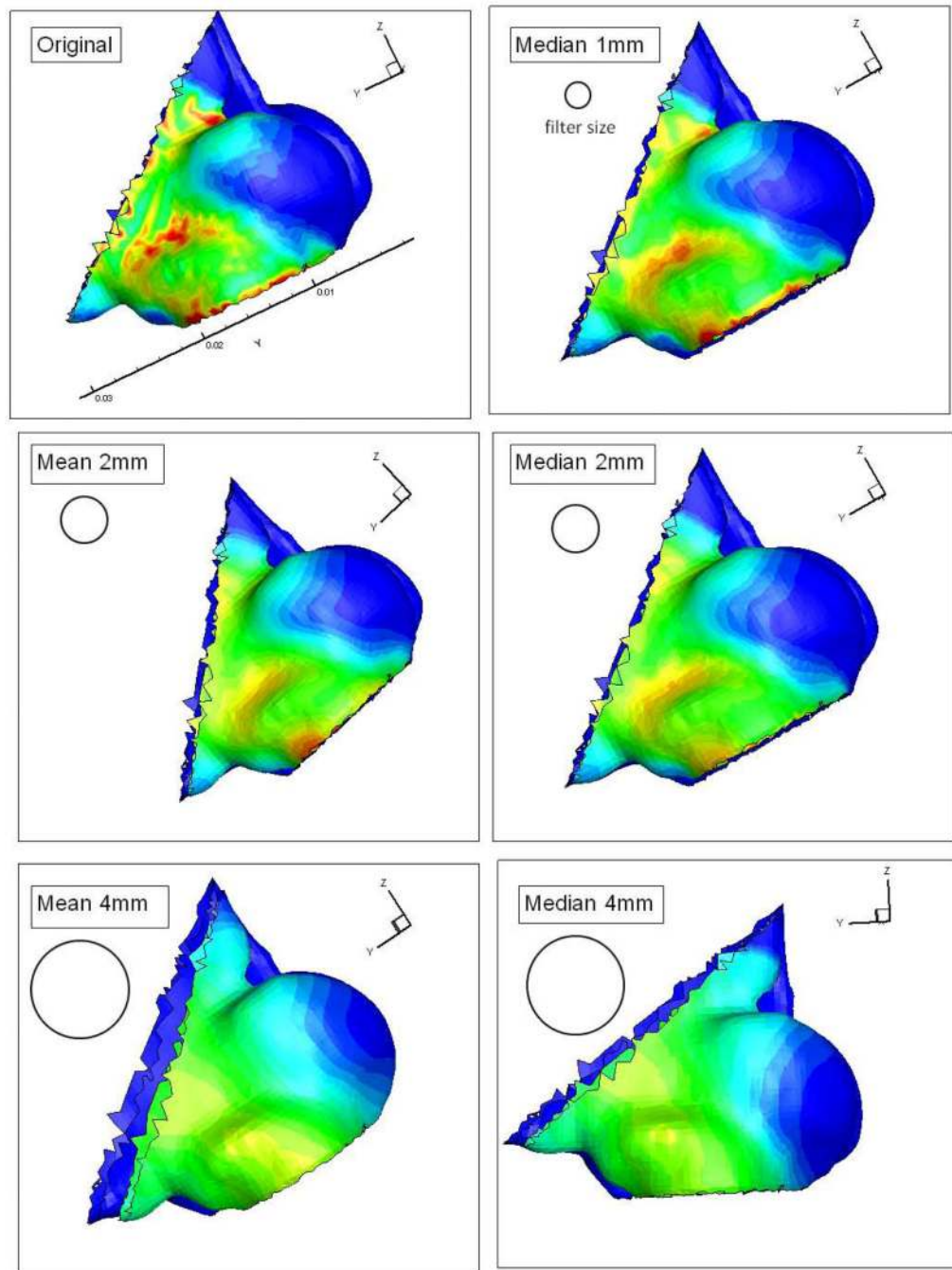


Figure 3. Effects of different spacial filters applied to surface heat loss, including 1mm, 2mm, and 4mm radius mean (moving average) and median filter in the nasal vestibule region of one subject.

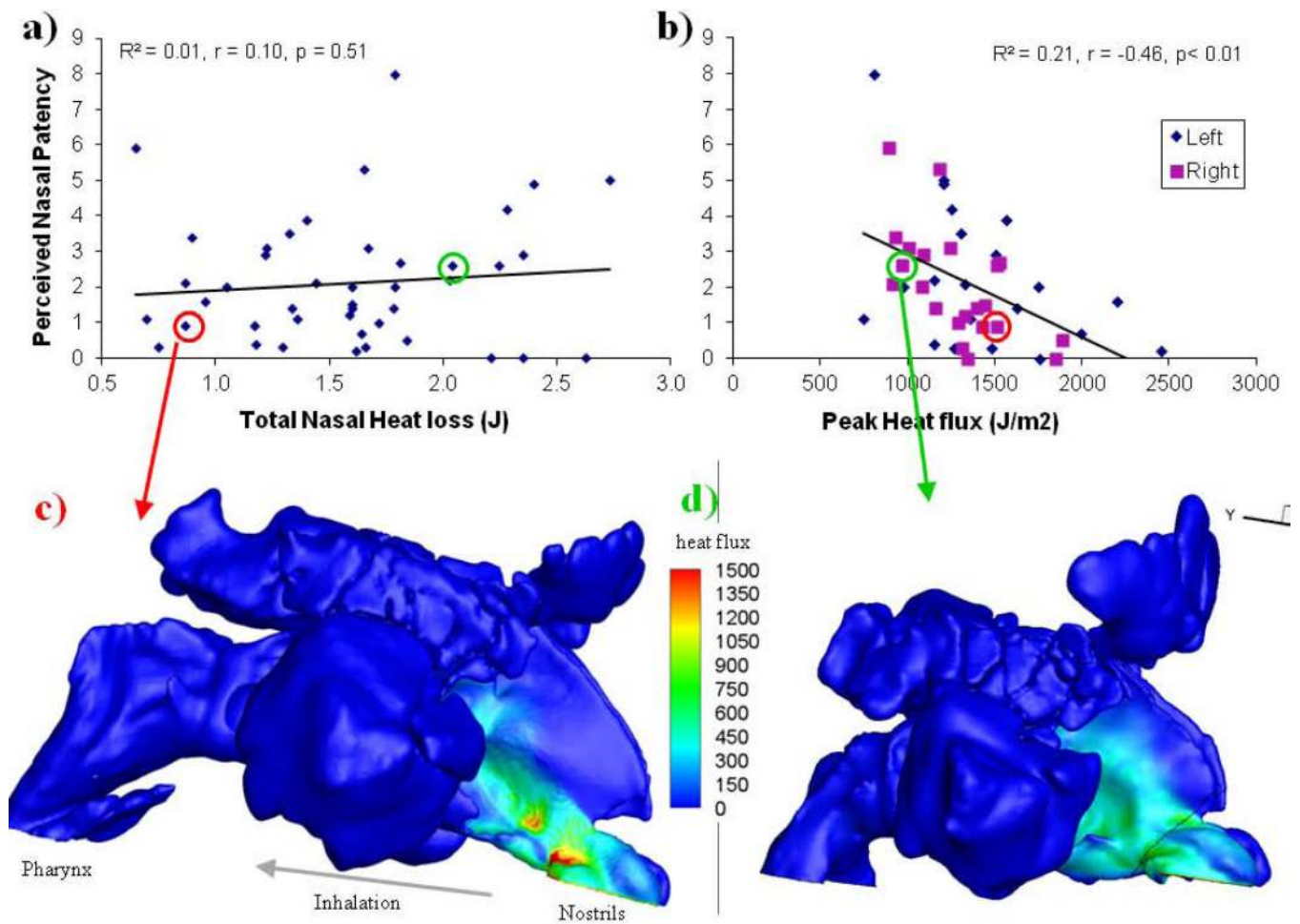


Figure 4. 22 healthy subjects rated unilateral nasal patency with a visual analogue scale (10 being completely congested, 0 being completely clear) under controlled room conditions; these ratings correlate significantly (Pearson correlation coefficient) with CFD simulated peak nasal mucosal heat loss post nasal vestibule (panel b), but not with total nasal heat loss (panel a). (c, d) Examples of simulated nasal heat loss for two subjects, which illustrate that it is possible to have low total nasal heat loss but high peak loss (panel c, red circled data points) and high total nasal heat loss but low peak flux (d, green circled data points).

Table 1

Pearson correlation matrix between variables.

| N=28 | Resistance (stimulation) | Patency | Peak heat loss (post vestibule) | MCA | Total Heat loss | Butanol lateralization threshold | Heat loss (nasal vestibule, CFD) |
|--------------------------------------|--------------------------|---------|---------------------------------|-----|-----------------|----------------------------------|----------------------------------|
| Nasal resistance (rhinomanometry) | 0.41 * | | | | 0.40 * | | 0.37 |
| Nasal resistance (CFD simulated) | | | | | 0.98 * | 0.40 | 0.60 * |
| Patency | | | -0.46 * | | | | |
| Peak heat loss (post vestibule, CFD) | | | | | | | |
| MCA (acoustic rhinometry) | | | | | 0.34 | 0.39 | 0.34 |
| Total Heat loss (CFD) | | | | | | 0.43 | 0.64 * |
| Butanol lateralization threshold | | | | | | | 0.51 * |

Values shown are those with correlation coefficients $r > 0.33$ (accounting for at least 10% of total variance) and significant at the level of $p < 0.05$.

Those with *, $p < 0.01$.

Among all independent variables, only the peak mucosal heat loss posterior to the nasal vestibule correlates significantly with patency ratings.

Table 2

Linear discriminant analysis (LDA) classification Matrix of predicted versus actual patency category and the success rate.

| Groups | Predicted Excellent Patency | Predicted Normal Patency | Predicted Obstructed Patency | Percent Correct |
|--------------------|------------------------------------|---------------------------------|-------------------------------------|------------------------|
| Excellent Patency | 17 | 1 | 0 | 94.44% |
| Normal Patency | 2 | 6 | 0 | 75% |
| Obstructed Patency | 0 | 0 | 2 | 100% |
| Total | 19 | 7 | 2 | 89.29% |

Table 3

Multivariate (Wilks Lambda) and Univariate (F) tests of equality of group means, probability value and Lambda for the six independent variables in LDA classification analysis.

| N=28 | Wilks' Lambda | F (2, 20) | P-VALUE | Partial Lambda |
|--------------------------------------|---------------|-----------|---------------|----------------|
| Nasal resistance (rhinomanometry) | 0.38 | 4.22 | 0.03* | 0.70* |
| Peak heat loss (post vestibule, CFD) | 0.50 | 8.71 | 0.002* | 0.53* |
| MCA (acoustic rhinometry) | 0.31 | 1.59 | 0.23 | 0.86 |
| Total nasal heat loss (CFD) | 0.31 | 1.79 | 0.19 | 0.85 |
| Butanol lateralization threshold | 0.38 | 4.17 | 0.03* | 0.71* |
| Heat loss (nasal vestibule, CFD) | 0.32 | 2.17 | 0.14 | 0.82 |

Wilk's Lambda is a multivariate equivalent of the ANOVA (F) test of mean differences in LDA, such that the smaller the lambda for an independent variable, the more that variable contributes to the discriminant function. The Lambda varies from 0 to 1, with 0 explaining 100% of the variability and 1 explaining 0% of the variability. Partial Lambda is a measure of how much variability is accounted for by each individual variable by itself while ignoring the contribution of the other variables. Here, peak heat loss (post vestibule) can explain the most variability by itself, followed by nasal resistance and butanol lateralization threshold.